Hindawi
Advances in Materials Science and Engineering
Volume 2020, Article ID 6804906, 11 pages
https://doi.org/10.1155/2020/6804906

Research Article

Experimental Study and Application of LASC Foamed Concrete to Create Airtight Walls in Coal Mines

Duo Zhang[1,2] **Weifeng Wang**[1,2] **Jun Deng**[1,2] **Hu Wen**[1,2] **and Xiaowei Zhai**[1,2]

[1]*School of Safety Science and Engineering, Xi'an University of Science and Technology, Xi'an, Shaanxi 710054, China*
[2]*Key Laboratory of Mine and Disaster Prevention and Control of Ministry of Education, Xi'an University of Science and Technology, Xi'an, Shaanxi 710054, China*

Correspondence should be addressed to Duo Zhang; zhangd@xust.edu.cn and Weifeng Wang; wangwf@xust.edu.cn

Received 7 October 2019; Revised 12 December 2019; Accepted 2 January 2020; Published 23 January 2020

Academic Editor: Francesco Ruffino

If an airtight wall in a coal mine leaks air, it may cause spontaneous combustion of residual coal in the gob and even cause a full-blown fire or gas explosion. In this study, we developed a new type of foamed concrete, low-alkalinity sulphoaluminate cement (LASC), to control air leakage. The performance of filling materials that were prepared by adding various dosages of foam to LASC was studied. The longer the curing period for the foam filling material of LASC, the better the crystallinity of the hydrated product. With an increasing foam dosage, the initial setting time gradually extends while the fluidity of the foam slurry decreases. The bubble rate of the filling material increases and the density decreases with increasing foam dosage. The compressive strength of the LASC filling material decreases with increasing foam dosage and increases with increasing curing time. In the LASC filling materials, the optimal volume ratio of foam dosage to gel slurry is 2. The crystallinity, initial gel time, and compressive strength of the LASC foaming materials are better than those of ordinary Portland cement (OPC) foaming materials. When the crossheading is filled with LASC foam cement, the deformation of the surrounding rock is less than 19 cm, and the air leakage prevention is better than that achieved with loess and fly-ash-cement foam. Thus, the proposed LASC foam material can be applied to the filling of the crossheading to efficiently prevent leakage in underground coal mines.

1. Introduction

Coal seam fires that are caused by air leakage are a serious threat to the operation of coal mining. Explosions due to gas, coal dust, and water coal gas and smoke poisoning cause interruptions in operations and may lead to casualties [1–3]. Spontaneous coal combustion is a major global disaster that leads to serious environmental pollution (Figure 1) [4–6]. In particular, the risk of spontaneous combustion of the gob in underground coal mines is greater [7, 8]. As shown in Figure 2, the special mining method used in Chinese coal mines determines that many crossheadings are left in the gob. Thus, building an airtight wall is an effective means of preventing spontaneous combustion of coal, which is caused by air leakage through the crossheadings [9, 10].

Limitations of materials and techniques have prevented the construction of airtight walls over recent decades. These limitations mainly include the following aspects. Reinforced concrete has high strength, but its elastic shape weakens, causing the wall or the surrounding coal body to fracture easily and thereby causing air leakage. To solve the problem of poor contact sealing, scholars have developed rigid polyurethane foam [11], polyurethane, and phenolic resin [12, 13]. These materials have good sealing properties but have disadvantages such as the release of toxic gases, significant costs, and high-temperature generation, which promotes oxidation of coal.

The development of new materials is critical for constructing high-quality airtight walls. Foam cement has interested several experts because of its low density, low thermal conductivity, low permeability, high expansibility, and high strength [14]. Ivanov et al. [15] and Siva et al. [16, 17] investigated the foaming properties of different types of foaming agents such as sodium lauryl sulphate. Deng et al.

(a) (b)

Figure 1: Environmental pollution caused by spontaneous combustion of coal. (a) Flue gas produced by spontaneous combustion. (b) Exposed open flame after peeling off the surface.

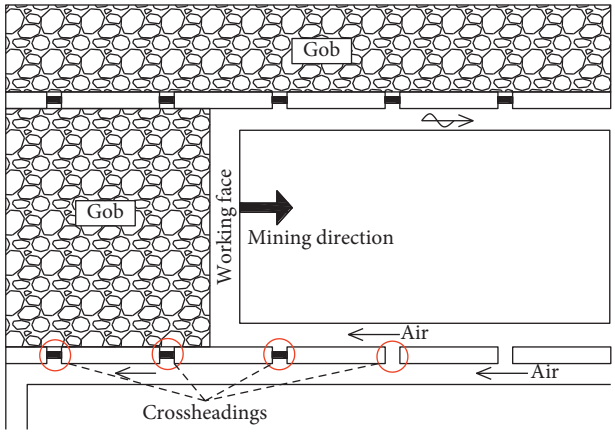

Figure 2: Schematic diagram of a quintessential manway in a Shenfu coalfield: each crossheading is 50 m.

[18] and Fan et al. [19] studied the influencing factors of foam stability. Lu et al. [20], Wang [21], and Zheng et al. [9] designed a foaming device and analyzed the effects of pressure and the flow of blowing agents on foam performance. Kearsley and Wainwright [22] studied the effect of porosity on the strength of foam concrete. Kearsley and Wainwright studied the effect of thermal conductivity and fly ash content on the compressive strength of foam concrete [23]. Jambor [24] and Tang [25] analyzed the effect of pore structure on the strength of foam concrete. Nambiar and Ramamurthy [26] studied the pore characteristics of foam concrete. Mohammadhosseini and Yatim [27] investigated the effect of waste polypropylene carpet fibers and palm oil fuel ash on the mechanical and microstructural properties of concrete exposed to high temperatures. Lim et al. [28] investigated the effects of waste ceramic powder on both the mechanical and microstructural properties of mortar. Böke et al. [29] and Wen et al. [30, 31] studied the method of preparing solidified foam filling materials using fly ash, and they analyzed the influence of factors such as the water-cement ratio and foaming multiple on the foam. The use of fly ash foam cement in plugging air leakages has greatly reduced coal dust pollution on the ground. Generally, the slump period of the coal and rock mass in the gob is five to eight days. The compressive strength of fly ash foam cement after seven days of curing is less than 2 MPa. This causes the shape change of the surrounding rock of the crossheading to be relatively larger, and the filling wall is easily fractured. Therefore, studying quick-setting, high-strength, solidified filling materials for foam cement that are appropriate for current coal mining technology is necessary.

Although many experts and scholars have conducted extensive research on OPC-based foam cement for coal mines, minimal attention has been paid to LASC foam cement, which has quick-setting and high-early-strength functions.

In this paper, the influence of foam dosage on the properties of LASC filling materials is mainly studied. The effects of foam dosage on the foam filling materials' microstructure, initial setting time, porosity, and compressive strength are presented. Its efficiency was utilized for No. 31411 working face of Halagou coal mine in 2018. Field industrial tests have shown that LASC has good sealing and compressive strength effects.

2. Material Selection and Preparation Method

OPC (P.O 42.5, Yulin Shanshui Cement Plant, Shaanxi Province, China) and LASC (L.SAC 42.5, Yulin Shanshui Cement Plant, Shaanxi Province, China) were selected for this study. The physical properties and chemical compositions of OPC and LASC are listed in Tables 1–4. Lauryl amidopropyl betaine ($C_{20}H_{40}N_2O_3$) and potassium monoalkyl phosphate ($C_{12}H_{25}OPO_3K_2$) were used as activators for the foaming agent and were mixed in a ratio of 7 : 3. Triethanolamine ($C_6H_{15}NO_3$) and oleic acid ($C_{18}H_{34}O_2$) were used as foam stabilizers and were mixed in a ratio of 1 : 1. The foaming agent and foam stabilizers were mixed in a ratio of 1 : 1. The foam was prepared according to procedures described in reference [9].

Table 1: Chemical composition of OPC (%).

CaO	SiO_2	Al_2O_3	Fe_2O_3	SO_3	MgO	TiO_2	K_2O	Na_2O
64.28	20.47	6.57	2.79	1.17	2.31	0.91	0.84	0.66

Table 2: Physical performance of OPC.

Fineness (0.08 mm, that formed a residue on square-hole sieve)	Apparent density (kg/m^3)	Initial setting time (min)	Final setting time (min)	Compressive strength (MPa)	
8%	3.06	139	375	1 d 12.8	28 d 46.7

Table 3: Chemical composition of LASC (%).

CaO	SiO_2	Al_2O_3	Fe_2O_3	SO_3	MgO	TiO_2
42.44	12.46	30.58	2.54	9.52	0.64	1.82

Table 4: Physical performance of LASC.

Apparent density (kg/m^3)	Initial setting time (min)	Final setting time (min)	Compressive strength (MPa)	
3.21	10	30	1 d 37.5	28 d 51

The process of preparing the inorganic solidified foam filling material is shown in Figure 3. A square-hole sieve with a diameter of 0.08 mm was used to screen out LASC and OPC cements, respectively. First, the gel slurry was prepared by mixing OPC or LASC with water in proportion. Subsequently, the foam was mixed with the gel slurry in proportion, and the foam slurry was uniformly prepared by stirring. Finally, the foam slurry was poured into the mold to prepare the foamed cement module ($100 \times 100 \times 100$ mm). Studies have shown that the strength of the cured foam cement is higher when the water-cement mass ratio is approximately 0.5 [30]. Therefore, the water-cement ratio used in this study was 0.5. The foam and gel slurry were mixed in a volume ratio. As shown in Table 5, the foam slurry was prepared by adding 1x, 2x, and 3x volumes of foam to the gel slurry, and these mixtures were designated as FGS 1, FGS 2, and FGS 3, respectively.

The microstructure and mineral phases of the foam filling material at the initial stage of molding (one and seven days) was tested using scanning electron microscopy (SEM, Hitachi S-4800N, Japan) and X-ray diffraction (XRD, Bruker-D8-Advance, copper target, step size: 0.03, Germany). The initial gel time of the foam filling material was measured, in accordance with Chinese Standard GB/T1346-2011, using a Vicat apparatus (Shandong Province, China). The compressive strength of the foam filling material was measured, in accordance with Chinese standard GB50107-2010, using an electronic universal testing machine (WDW-100E, Jiangsu Province, China).

3. Effect of Foam Dosage on Microscopic Properties of Solidified Filling Materials

3.1. SEM Experimental Study on Solidified Filling Materials. To study the effect of foam dosage on the hydration products of the solidified filling materials, we prepared the foam filling materials according to Table 5 and Figure 3, using OPC and LASC, respectively. The morphology of the hydrated product was obtained at a magnification of 12000x, and the results are shown in Figures 4–7.

As shown in Figure 4(a), when the OPC gel slurry was cured for one day with 1x foam dosage, a large number of fibers and network-like morphological products formed in the material, which were considered to be calcium silicate hydrate (C-S-H) by comparison to the morphology of each mineral hydration product of cement [32, 33]. In Figures 4(b) and 4(c), there was a needle-like product that was considered to be ettringite (AFt) [34]. Figure 4 also shows that the space between the hydration products of the filling material gradually increased as the amount of foam increased. Figure 5 shows that there were hexagonal prismatic AFt and C-S-H fiber networks in the LASC solidified foam cement filling material for the different foam dosages. Additionally, there was a clear needle-shaped AFt, as shown in Figure 5(c).

As illustrated in Figures 6(a) and 6(b), when the OPC gel slurry was cured for seven days with 1x and 2x foam dosages, C-S-H fiber networks and needle bar AFt formed in the material, and the AFt was wrapped by the C-S-H. The AFt shown in Figure 6(c) was completely wrapped by the C-S-H. We found that the longer the curing time, the better the degree of crystallization of the material, by comparing the SEM images of the OPC gel slurry foam filling materials that were cured for one and seven days. As shown in Figures 7(a) and 7(b), when the LASC gel slurry was cured for seven days with the 1x and 2x foam dosages, hexagonal flaky calcium sulphoaluminate (AFm), C-S-H, and AFt formed in the material. Figure 7(b) also shows hexagonal plate-like $Ca(OH)_2$. C-S-H and Aft were present, as shown in Figure 7(c).

Figure 3: Schematic diagram of the preparation of the filling material.

Table 5: Mixing ratio of foam and gel slurry.

Water-cement ratio (by mass)	Volume ratio of foam to gel slurry		
0.5	FGS 1 1	FGS 2 2	FGS 3 3

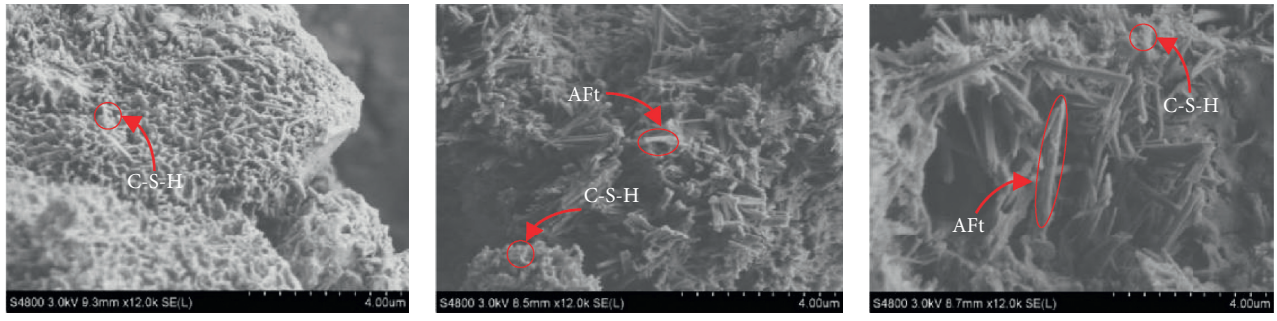

(a) (b) (c)

Figure 4: SEM image of OPC cured foam filling material when molded for one day. (a) FGS 1. (b) FGS 2. (c) FGS 3.

The crystallinity of the hydrated product of the LASC foam cement filling material was found to be better than that of the OPC foam cement filling material for the same curing period. The longer the curing time for the solidified foam filling material of the same type of cement, the better the crystallinity of the hydrated product, which means that the longer the curing, the more complete the hydration of the material.

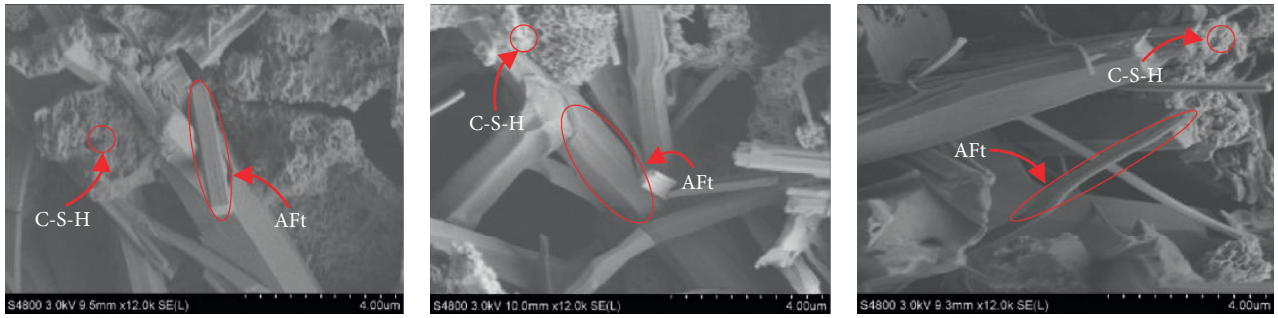

(a) (b) (c)

Figure 5: SEM image of LASC cured foam filling material when molded for one day. (a) FGS 1. (b) FGS 2. (c) FGS 3.

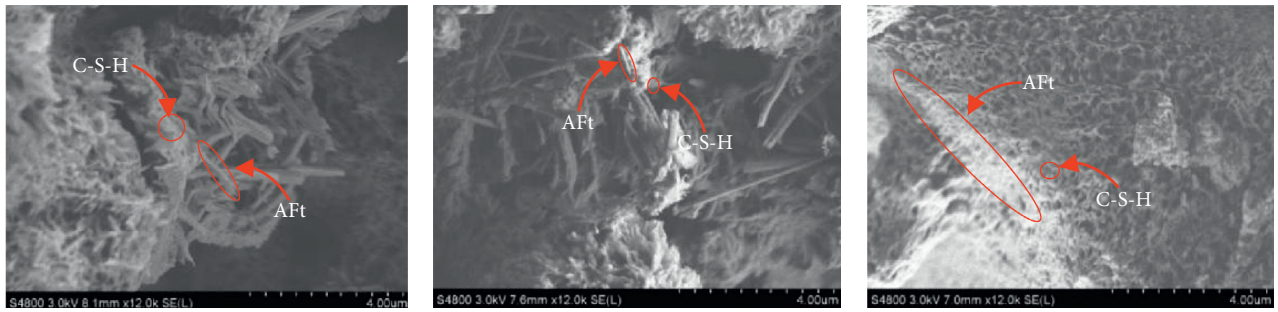

(a) (b) (c)

Figure 6: SEM image of OPC cured foam filling material when molded for seven days. (a) FGS 1. (b) FGS 2. (c) FGS 3.

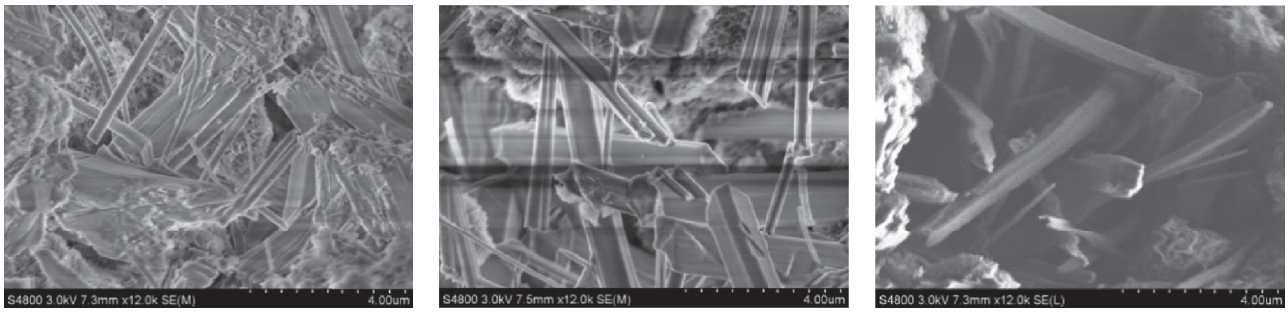

(a) (b) (c)

Figure 7: SEM image of LASC cured foam filling material when molded for seven days. (a) FGS 1. (b) FGS 2. (c) FGS 3.

3.2. XRD Experimental Study on Solidified Filling Materials. To study the influence of foam dosage on the solidified filling materials, we prepared the foam filling materials according to the data in Table 5 and Figure 3 using OPC and LASC, respectively. The results are shown in Figures 8 and 9.

As shown in Figure 8, the hydration products of the OPC foam slurry when solidified for one day included $3CaO{\cdot}Al_2O_3{\cdot}3CaSO_4{\cdot}32H_2O$, $Ca(OH)_2$, $3CaO{\cdot}SiO_2$, and $CaCO_3$. The hydration products of the LASC foam slurry for the same condition included $3CaO{\cdot}Al_2O_3{\cdot}3CaSO_4{\cdot}32H_2O$, $CaSO_2$, $2CaO{\cdot}SiO_2$, and $CaCO_3$. As illustrated in Figure 9, the hydration products of the OPC foam slurry when solidified for seven days included $3CaO{\cdot}Al_2O_3{\cdot}3CaSO_4{\cdot}32H_2O$, $Ca(OH)_2$, and $CaCO_3$. The hydration products of the LASC foam slurry for the same condition included $3CaO{\cdot}Al_2O_3{\cdot}3CaSO_4{\cdot}32H_2O$ and $CaCO_3$.

4. Effect of Foam Dosage on Properties of Solidified Filling Materials

4.1. Effect of Foam Dosage on the Initial Gel Time and Fluidity. To explore the effects of the foam dosage on the solidified foam filling material, we designed the experiments as shown in Table 5 and Figure 3. We adjusted the dosage of the foam and measured the initial gel time and fluidity [35], as presented in Figure 10.

Figure 10 indicates that the larger the foam dosage, the longer the initial setting time was. This was because the foam

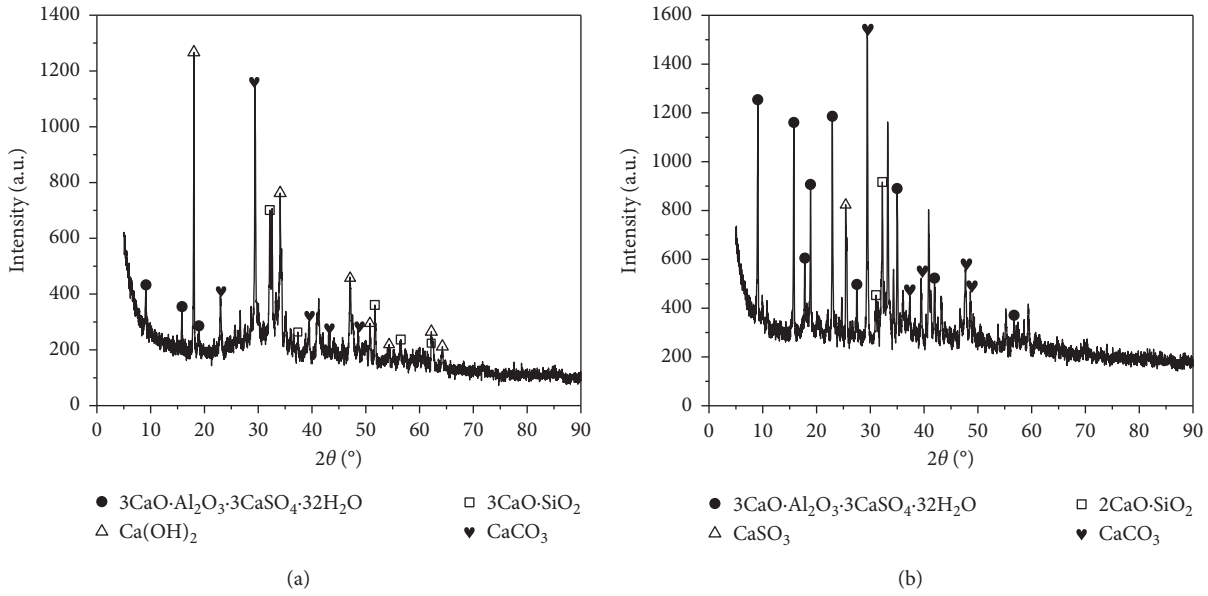

Figure 8: XRD pattern of cured foam filling material when molded for one day. (a) OPC. (b) LASC.

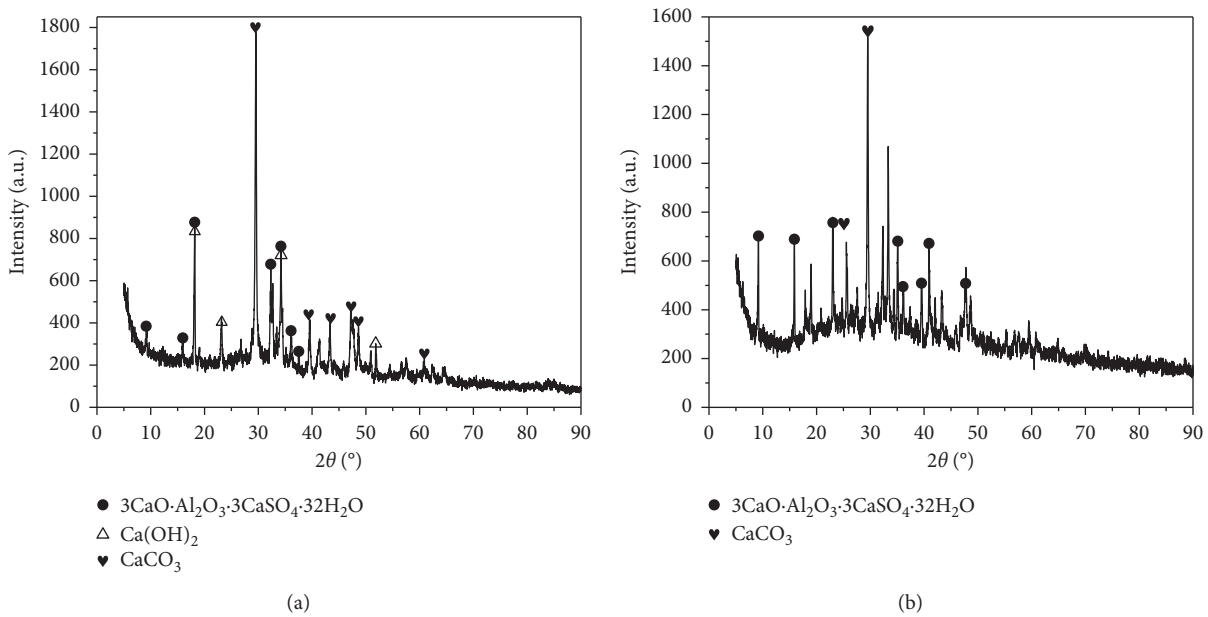

Figure 9: XRD pattern of cured foam filling material when molded for seven days. (a) OPC. (b) LASC.

has poor gas permeability and good water retention, which hindered the hydration effect. The minimum and maximum initial setting times of the OPC foam slurry under the experimental conditions were 7.0 and 12.7 h, respectively. The minimum and maximum initial setting times for the LASC foam slurry were 3.0 and 3.9 h, respectively. Clearly, the initial setting time of LASC was less than that of OPC. This was because the Al_2O_3 content of LASC is higher than that of OPC and the hydration rate of $3CaO{\cdot}Al_2O_3$ and $4CaO{\cdot}Al_2O_3{\cdot}Fe_2O_3$ is greater than that of $3CaO{\cdot}SiO_2$ and β-$2CaO{\cdot}SiO_2$ [36]. Additionally, Figure 10 shows that the fluidity of the foam slurry decreased as the foam content increased. This was because the fluidity of the foam was less than that of the slurry [9].

4.2. Effect of Foam Dosage on the Material Bubble Rate and Density. Studies have shown that the pore structures of foam filling materials differ depending on the types of cement and doses of the foam [37]. According to reference [38], the bubble rate of the solidified filling material can be calculated using equation (1). The results are shown in Figures 11 and 12.

$$p = \left(1 - \frac{\rho_m}{\rho_0}\right) \times 100\%, \quad (1)$$

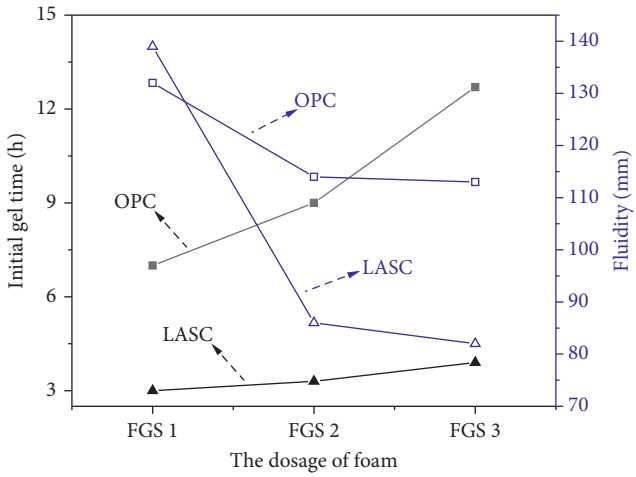

Figure 10: Initial setting time and fluidity of filling materials under different foaming dosage.

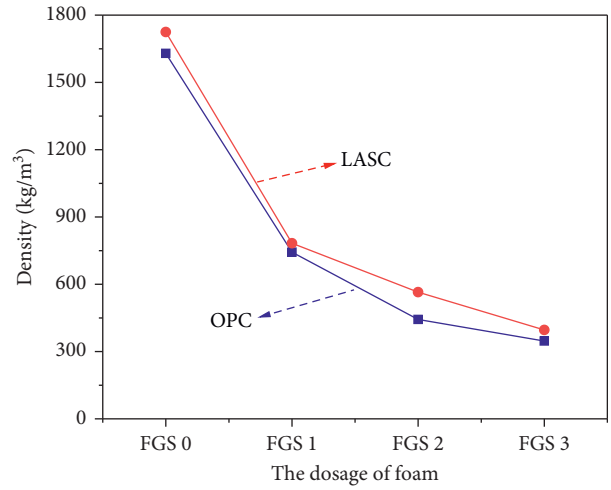

Figure 12: Foam dosage and density of the filling material. FGS 0 is ρ_0, which is the material density after solidification of cement.

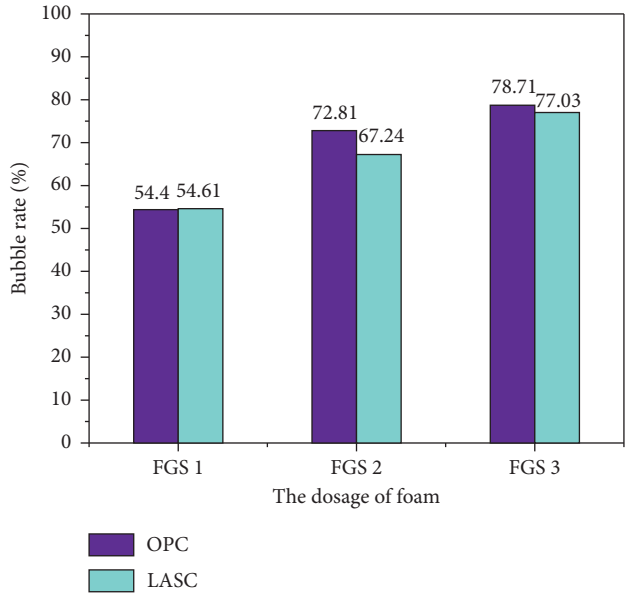

Figure 11: Foam dosage and bubble rate of the filling material.

where p is the bubble rate of the solidified foam cement material (%), ρ_m is the density of the solidified foam cement material (g/cm^3), and ρ_0 is the density of the solidified cement material (g/cm^3).

Figure 11 shows that the bubble rate increased with increasing foam dosage. For the OPC solidified foam cement filling material, the bubble rate of the 2x foam dosage was 18.31% higher than the 1x foam dosage; the bubble rate of 3x dosage was 5.90% higher than the 2x dosage. For the LASC solidified foam cement filling material, the bubble rate at the 2x foam dosage was 12.63% higher than that at the 1x amount; the bubble rate at the 3x dosage was 9.79% higher than that at the 2x dosage.

From Figure 12, we can see that the density of the solidified foam filling material of the LASC was slightly higher than that of the OPC material. The density decreased with increasing foam dosage. This was because the dry density of the filling material decreases with an increase in the foam dosage, whereas the bubble rate depicts an opposite trend [22].

4.3. Effect of Foam Dosage on Compressive Strength of the Materials. According to the data in Figure 3 and Table 5, a 100 × 100 × 100 mm foamed cement test piece was prepared. The compressive strength of the foamed cement filling materials for one and seven days of molding was tested using a WDW-100E electronic universal testing machine. The experiment adopted an equal-displacement single-axis compression method, where the speed was 4.0 mm/min, maximum pressure was 100 kN, displacement resolution was 0.001 mm, and stepless speed regulation range was 0.005–500 mm/min. Pressurization was stopped when the material was broken, and the deformation was greater than 30 mm. The experimental results are shown in Figures 13 and 14.

As can be seen, under the same conditions, the longer the curing time, the greater the compressive strength owing to the more stable crystal structure of the hydration product [30]. This was because the higher the foam dosage, the higher the bubble rate of the solidified foam cement, the better the compressibility, and the greater the yield strength [39]. When the compressive strength reached the peak, it steadily fluctuated on a horizontal line or decreased gradually, which reflected the compressible properties of the cured foam filling material. Additionally, Figures 13 and 14 show that the compressive strength of the filling material declined steeply after reaching the peak value, and the larger the foaming dosage, the larger the displacement value corresponding to the sudden decline in stress. The reasons for this phenomenon may be as follows. (1) The curing period was short, and the hydration was not complete. (2) The filling material entered the stage of plastic deformation. (3) Nonpenetrating cracks appeared in the test piece during the pressure-bearing process, and the material contained

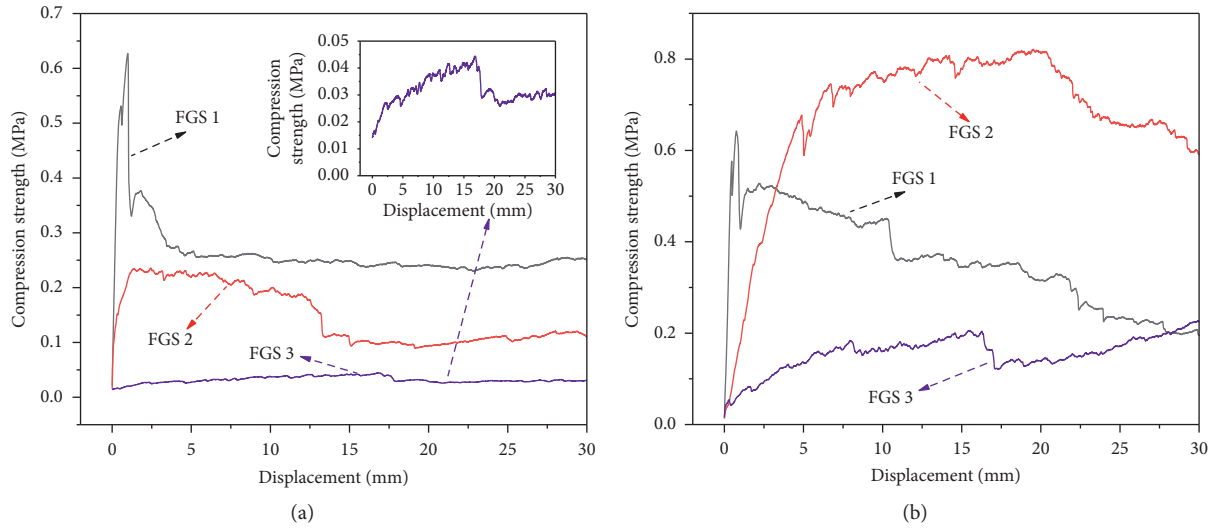

Figure 13: Compressive strength-displacement curve for OPC foam cement filling materials. (a) 1 d, (b) 7 d.

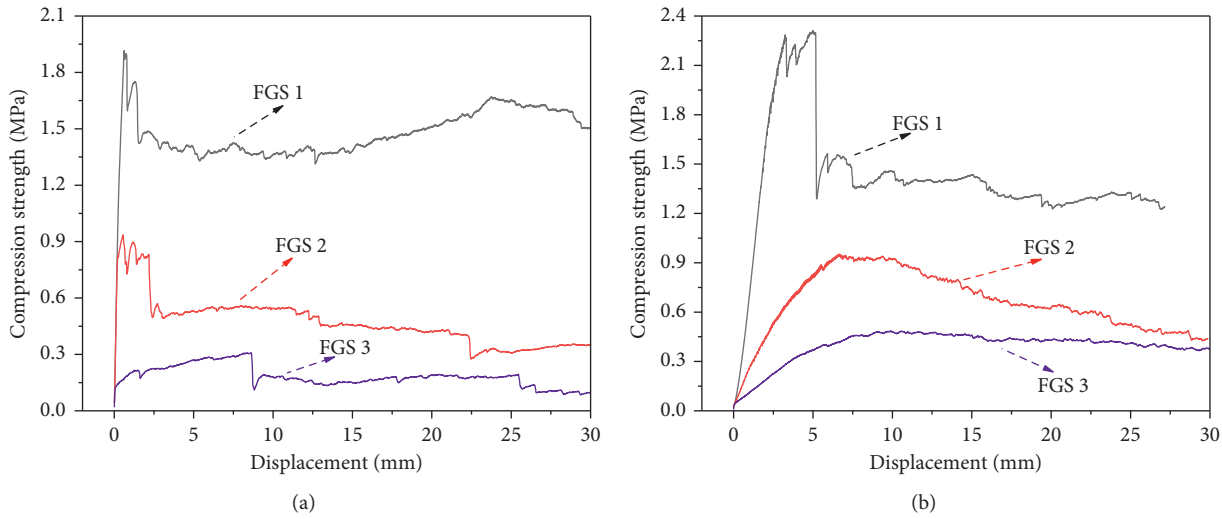

Figure 14: Compressive strength-displacement curve for LASC foam cement filling materials. (a) 1 d, (b) 7 d.

$Ca(OH)_2$. The compressive strength of the OPC solidified foam filling material was lower than that of the LASC solidified foam filling material under the same foam dosage and curing period. This was because the crystallinity of the LASC material is superior to that of the OPC material. Under the same cement and foam dosage conditions, the longer the curing period of the filling material, the greater the compressive strength. This was because the degree of hydration and the crystallinity of the product of hydration are directly proportional to the curing period.

5. Field Application Analysis

In 2018, LASC solidified foam filling technology was utilized for No. 31411 working face of the Halagou coal mine in the Shendong Mining Area. The water-ash mass ratio of the material was 0.50 and the volume ratio of the foam to gel slurry was 2. The perfusion was performed using a self-developed ZMJ-F type pulping machine. The pressure applied by the machine was 0.60 MPa, and the perfusion flow rate of the slurry pump was 16.00 m^3/h. The specific process flow is shown in Figure 15. Figures 16 and 17 show the shape variables of the crossheading after filling and the O_2 concentration of the gob, respectively.

As illustrated in Figure 16, the displacement of the surrounding rock in the crossheading after filling with LASC foam material was small, and it essentially became stable after 22 d. The cumulative displacement of the top and bottom plates was 18.90 cm, and the cumulative displacement of the coal walls on both sides was 17.10 cm. No cracks were found on the filling wall during the observation period. As seen in Figure 17, when the LASC foaming cement was used to fill the crossheading, the

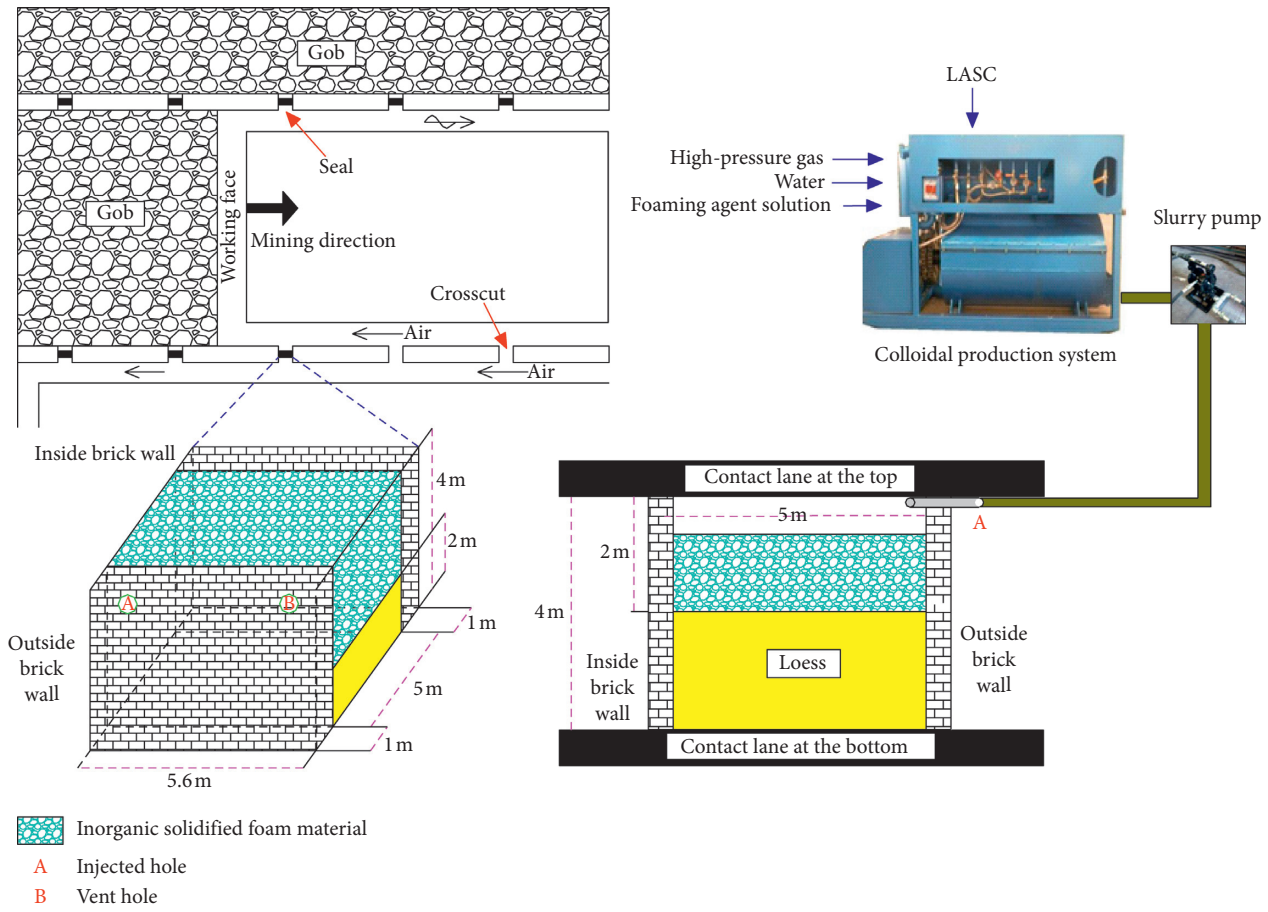

Figure 15: Schematic diagram of LASC curing foam cement filling process.

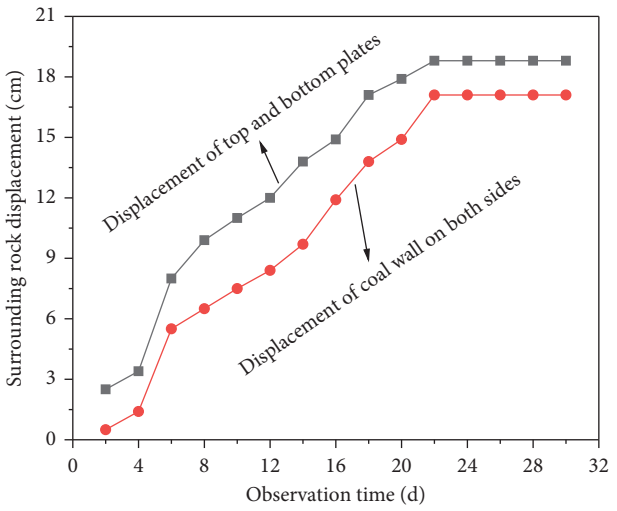

Figure 16: Shape variation of the surrounding rock around the crossheading.

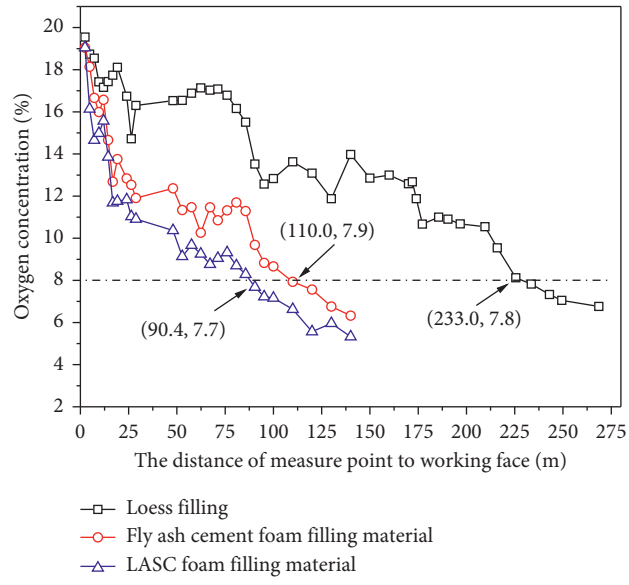

Figure 17: Concentrations of oxygen in a gob space.

oxygen concentration at 90.40 m on the inlet side of the gob reduced to 7.70%. Compared with loess and fly ash, the LASC foam cement material significantly reduced the extent of the hazardous areas of oxidation and spontaneous combustion in the gob [9]. The displacement of the surrounding rock and the O_2 concentration of the gob indicate that the LASC solidified foam exhibited a good filling effect.

6. Conclusions

A new coal mine roadway filling and sealing material was studied, and the performance of the LASC solidified foam filling material was tested. The main conclusions are as follows:

(1) For the same curing period (1 or 7 d), the crystallinity of the hydrated product of the LASC solidified foam cement filling material is better than that of OPC solidified foam cement filling material. The crystallinity of the hydrated product of the LASC foam filling material molded for 7 d is better than that for 1 d.

(2) The larger the foam dosage, the longer the initial setting time of the foam slurry. The minimum and maximum initial setting times of the LASC foam slurry were 7.0 and 12.7 h, respectively. The fluidity of the foam slurry decreases as the foam dosage increases. The minimum and maximum fluidity of the LASC foam slurry were 82 and 139 mm, respectively.

(3) When FGS is 2, the combined effect of parameters such as bubble rate, density, and compressive strength of the LASC foam filling material is better than for OPC.

(4) The crystallinity, initial gel time, and compressive strength of the LASC foaming material are better than those of the OPC foaming material.

(5) The application results show that the variation in the surrounding rock shape and the oxygen concentration in the gob are significantly reduced when the crossheading is filled with the LASC foam material. The effect of the LASC solidified foam cement filling in preventing air leakage is better than that of fly ash cement and loess. Therefore, the proposed filling material of LASC has broad application prospects owing to its good performance and suitability for large-area fillings.

Data Availability

The data used to support the findings of this study are available from the corresponding author upon request.

Conflicts of Interest

The author(s) declare that they have no conflicts of interest.

Authors' Contributions

Duo Zhang and Weifeng Wang contributed equally to this work.

Acknowledgments

The project was supported by the National Natural Science Foundation of China (grant nos. 51904234 and 51974240) and the Key R&D Program of Shaanxi Provincial (grant number 2017ZDCXL-GY-01-02-03).

References

[1] J. Deng, Y. Xiao, Q. Li, J. Lu, and H. Wen, "Experimental studies of spontaneous combustion and anaerobic cooling of coal," *Fuel*, vol. 157, pp. 261–269, 2015.

[2] C. Kuenzer and G. B. Stracher, "Geomorphology of coal seam fires," *Geomorphology*, vol. 138, no. 1, pp. 209–222, 2012.

[3] J.-j. Wu and X.-c. Liu, "Risk assessment of underground coal fire development at regional scale," *International Journal of Coal Geology*, vol. 86, no. 1, pp. 87–94, 2011.

[4] X. Hu, S. Yang, X. Zhou, Z. Yu, and C. Hu, "Coal spontaneous combustion prediction in gob using chaos analysis on gas indicators from upper tunnel," *Journal of Natural Gas Science and Engineering*, vol. 26, pp. 461–469, 2015.

[5] Z. Song and C. Kuenzer, "Coal fires in China over the last decade: a comprehensive review," *International Journal of Coal Geology*, vol. 133, pp. 72–99, 2014.

[6] J. Deng, C. Lei, Y. Xiao et al., "Determination and prediction on "three zones" of coal spontaneous combustion in a gob of fully mechanized caving face," *Fuel*, vol. 211, pp. 458–470, 2018.

[7] B.-t. Qin, Q.-g. Sun, D.-m. Wang, L.-l. Zhang, and Q. Xu, "Analysis and key control technologies to prevent spontaneous coal combustion occurring at a fully mechanized caving face with large obliquity in deep mines," *Mining Science and Technology (China)*, vol. 19, no. 4, pp. 446–451, 2009.

[8] C. Lei, J. Deng, K. Cao et al., "A comparison of random forest and support vector machine approaches to predict coal spontaneous combustion in gob," *Fuel*, vol. 239, pp. 297–311, 2019.

[9] X. Zheng, D. Zhang, and H. Wen, "Design and performance of a novel foaming device for plugging air leakage in underground coal mines," *Powder Technology*, vol. 344, pp. 842–848, 2019.

[10] L. Liu and F. B. Zhou, "A comprehensive hazard evaluation system for spontaneous combustion of coal in underground mining," *International Journal of Coal Geology*, vol. 82, no. 1-2, pp. 27–36, 2010.

[11] Y. Lu, "Laboratory study on the rising temperature of spontaneous combustion in coal stockpiles and a paste foam suppression technique," *Energy & Fuels*, vol. 31, no. 7, pp. 7290–7298, 2017.

[12] M. S. Yun and W. I. Lee, "Analysis of bubble nucleation and growth in the pultrusion process of phenolic foam composites," *Composites Science and Technology*, vol. 68, no. 1, pp. 202–208, 2008.

[13] B. T. Qin and D. M. Wang, "Present situation and development of mine fire control technology," *China Safety Science Journal*, vol. 12, pp. 80–85, 2007.

[14] X. Ni and N. E. Pereira, "Parameters affecting fluid dispersion in a continuous oscillatory baffled tube," *AICHE Journal*, vol. 46, no. 1, pp. 37–45, 2000.

[15] R. A. Ivanov, O. A. Soboleva, M. G. Chernysheva, and G. A. Badun, "Adsorption and distribution of components of cocoamidopropyl betaine-lysozyme mixtures in water/octane system," *Colloid Journal*, vol. 76, no. 3, pp. 319–326, 2014.

[16] M. Siva, K. Ramamurthy, and R. Dhamodharan, "Sodium salt admixtures for enhancing the foaming characteristics of sodium lauryl sulphate," *Cement and Concrete Composites*, vol. 57, pp. 133–141, 2015.

[17] M. Siva, K. Ramamurthy, and R. Dhamodharan, "Development of a green foaming agent and its performance evaluation," *Cement and Concrete Composites*, vol. 80, pp. 245–257, 2017.

[18] Q. Deng, H. Li, C. Li, W. Lv, and Y. Li, "Enhancement of foamability and foam stability induced by interactions between a hyperbranched exopolysaccharide and a zwitterionic surfactant dodecyl sulfobetaine," *RSC Advances*, vol. 5, no. 76, pp. 61868–61875, 2015.

[19] Z. Fan, Y. Li, C. Ding, M. Zhu, and J. Du, "Effects of polymer on foam stability," *Special Oil & Gas Reservoirs*, vol. 20, no. 6, pp. 102–104, 2013.

[20] X. Lu, H. Zhu, and D. Wang, "Investigation on the new design of foaming device used for dust suppression in underground coal mines," *Powder Technology*, vol. 315, pp. 270–275, 2017.

[21] H. Wang, D. Wang, Y. Tang, B. Qin, and H. Xin, "Experimental investigation of the performance of a novel foam generator for dust suppression in underground coal mines," *Advanced Powder Technology*, vol. 25, no. 3, pp. 1053–1059, 2014.

[22] E. P. Kearsley and P. J. Wainwright, "The effect of porosity on the strength of foamed concrete," *Cement and Concrete Research*, vol. 32, no. 2, pp. 233–239, 2002.

[23] E. P. Kearsley and P. J. Wainwright, "Ash content for optimum strength of foamed concrete," *Cement and Concrete Research*, vol. 32, no. 2, pp. 241–246, 2002.

[24] J. Jambor, "Pore structure and strength development of cement composites," *Cement and Concrete Research*, vol. 20, no. 6, pp. 948–954, 1990.

[25] L. P. Tang, "A study on the quantitative relationship between strength and pore size distribution of porous materials," *Cement and Concrete Research*, vol. 16, no. 1, pp. 87–96, 1986.

[26] E. K. K. Nambiar and K. Ramamurthy, "Air-void characterisation of foam concrete," *Cement and Concrete Research*, vol. 37, no. 2, pp. 221–230, 2007.

[27] H. Mohammadhosseini and J. M. Yatim, "Microstructure and residual properties of green concrete composites incorporating waste carpet fibers and palm oil fuel ash at elevated temperatures," *Journal of Cleaner Production*, vol. 144, pp. 8–21, 2017.

[28] N. H. A. S. Lim, H. Mohammadhosseini, M. M. Tahir, M. Samadi, and A. R. M. Sam, "Microstructure and strength properties of mortar containing waste ceramic nanoparticles," *Arabian Journal for Science & Engineering*, vol. 43, no. 10, pp. 5305–5313, 2018.

[29] N. Böke, G. D. Birch, S. M. Nyale, and L. F. Petrik, "New synthesis method for the production of coal fly ash-based foamed geopolymers," *Construction and Building Materials*, vol. 75, pp. 189–199, 2015.

[30] H. Wen, D. Zhang, Z. J. Yu, X. Zheng, S. Fan, and B. Laiwang, "Experimental study and application of inorganic solidified foam filling material for coal mines," *Advances in Materials Science and Engineering*, vol. 2017, Article ID 3419801, 13 pages, 2017.

[31] H. Wen, S. X. Fan, D. Zhang et al., "Experimental study and application of a novel foamed concrete to yield airtight walls in coal mines," *Advances in Materials Science and Engineering*, vol. 2018, Article ID 9620935, 13 pages, 2018.

[32] C. Hu, Y. Han, Y. Gao, Y. Zhang, and Z. Li, "Property investigation of calcium-silicate-hydrate (C-S-H) gel in cementitious composites," *Materials Characterization*, vol. 95, pp. 129–139, 2014.

[33] J. J. Chen, L. Sorelli, M. Vandamme, F. J. Ulm, and G. Chanvillard, "A coupled nanoindentation/SEM–EDS study on low water/cement ratio Portland cement paste: evidence for C–S–H/$Ca(OH)_2$ nanocomposites," *Journal of the American Ceramic Society*, vol. 93, no. 5, pp. 1484–1493, 2010.

[34] J. Jiang, Z. Lu, Y. Niu, and J. Li, "Investigation of the properties of high-porosity cement foams containing epoxy resin," *Construction and Building Materials*, vol. 154, pp. 115–122, 2017.

[35] W. Wang, G. L. Dai, and S. B. Nie, "Research on performance of grouting plugging material for inhibition of coal spontaneous combustion," *Journal of Safety Science and Technology*, vol. 10, no. 11, pp. 107–112, 2014.

[36] B. T. Qin and Y. Lu, "Experimental research on inorganic solidified foam for sealing air leakage in coal mines," *International Journal of Mining Science and Technology*, vol. 23, no. 1, pp. 151–155, 2013.

[37] A. E. Pramono, A. Zulfia, and J. W. Soedarsono, "Effect of HP process temperature on the density and porosity of Carbon-Carbon composites made of coal waste powder," *Journal of Materials Science and Engineering*, vol. 1, no. 3, pp. 316–322, 2011.

[38] C. J. Shao, Y. F. Xu, B. Chen et al., "Experimental study of strength characteristics of foam concrete," *Science Technology and Engineering*, vol. 16, no. 31, pp. 270–274, 2016.

[39] C. Lian, Y. Zhuge, and S. Beecham, "The relationship between porosity and strength for porous concrete," *Construction and Building Materials*, vol. 25, no. 11, pp. 4294–4298, 2011.